Physically-Based Haptic Synthesis

Vincent Hayward
Haptics Laboratory
McGill University, Montréal, Canada

Draft Chapter (September 2007) to appear in
Haptic Rendering: Foundations, Algorithms and Applications,
M. Lin and M. Otaduy (eds.), A K Peters, Ltd. (2008), pp. 297–309.

1 Introduction

The phrase "haptic rendering" was introduced by Salisbury *et al.* [1995] to designate a set of "algorithms for generating the force of interaction with virtual objects". In this seminal paper many of the key issues associated with the implementation of virtual mechanical environments were first described. Here, we would like to comment on the concept of "haptic synthesis", a set of algorithms designed to reduce the amount of online computations to a small and predictable amount, and yet able to synthesize signals which are physically accurate. The desire for a fixed, reduced amount of computation isn't primarily motivated by the limitations of today's microprocessors, but rather by basic facts about the physics of mechanical interaction between the macroscopic objects of interest in virtual reality simulations.[1]

This chapter discusses a set of algorithms to reconstruct interaction forces between virtual objects in a physically accurate manner. They must be fast enough to minimize the creation of spurious energy resulting from the discrete-time realization of displacement-to-force relationships. The most fundamental is an algorithm to compute the force of friction. Another algorithm is then described for sharp cutting, a close cousin of friction because of its dissipative nature. Synthesis of the nonlinear deformation response of arbitrary bodies is then considered. Textural effect are discussed in terms of small perturbations to the nominal signal. Finally, a simple shock synthesis technique based on Hertzian contacts is described. The haptic synthesis algorithms described in this chapter can be regarded as building blocks for a complete rendering system, and used together with other algorithms presented in this book.

Long ago it was noticed that when simulating an elastic element with a haptic device where the manipulandum position is measured and the returned force is commanded, the interaction has a tendency to break into a limit cycle. A limit cycle rather than a divergence generally occurs since, typically, there are nonlinear elements in the system. Colgate and Schenkel [1994] attributed this to delay introduced by the sampling and computation of the virtual environment. By elegant application of the small gain theorem, they found a condition for passivity: $\mathcal{B} > (\sigma\mathcal{T}/2)+b$. In this expression, $\mathcal{B}$ is the device viscous damping, $\mathcal{T}$ the delay equated to one sample period, and σ, b are the simulated stiffness and damping coefficients respectively. They concluded that achievable damping is not dependent on the sampling rate, nevertheless achievable stiffness is.

A commonly adopted approach to deal with this problem is the "virtual coupling" method described by Adams and Hannaford [1999] that limits the interaction impedance to an achievable value. Other approaches include deadbeat control ideas [12] or predictive-sample-hold [11], methods which invariably increase the complexity and the amount of computations required from sample to sample.

Suppose that the virtual environment to be simulated is a spring deflected by d. We may view sampling and reconstruction as a form of generative hysteresis where the force response of the computer simulation lags behind displacement. For a zero-order hold, we can evaluate the energy gained from sample to sample as the area described by the force trajectory branching off from the displacement trajectory until they meet again after one sample period, see Figure 1, that is $1/2\,\Delta f\,\Delta d \approx 1/2\,\sigma(\Delta d)^2$.

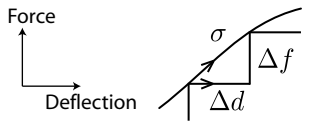

Figure 1: Response Branching.

For energy to decrease at all times, the incremental potential energy gained by delaying the simulation of the spring by one period should be smaller than the energy lost in viscosity by the manipulandum moving at average velocity v during the same period, that is: $\mathcal{B}v\Delta d \approx \mathcal{B}(\Delta d)^2/\mathcal{T}$

[1] The four first sections of this chapter are adapted from a paper published in the Proceedings of the 8th International IFAC Symposium on Robot Control, SYROCO 2006 Bologna (Italy) (Keynote paper). This material is used with permission of the International Federation of Automatic Control.

which gives: $\mathcal{B} \gtrsim 1/2\,\sigma\mathcal{T}$. This is equivalent to Colgate's expression. What is more, this reasoning does not require any particular assumption about the simulated environment so we can generalize this to $\mathcal{B}(t) \gtrsim 1/2\,\sigma(d,t)\mathcal{T}$.[2] In fact in [23] a theorem is indicated that guarantees the existence of $\mathcal{T}$ for the passive synthesis of a wide class of nonlinear, multidimensional virtual environments.

Recently, a similar expression was obtained to relate the dissipation due to dry friction with position measurement quantization. Limit cycles can be prevented if there is sufficient friction, namely, if $f_\mathrm{f} \geq 1/2\,\sigma\,\delta$, where δ is the position quantum and f_f the friction force [1, 8]. To derive this expression, consider that the effect of quantization is to offset the force update by at most δ. As in the previous paragraph we require friction to dissipate the energy gained from an error of at least one position quantum. The area under the branching triangle is $1/2\,\sigma\,\delta^2$. The energy lost to friction between two updates must be greater, $f_\mathrm{f}\,\delta \geq 1/2\,\sigma\,\delta^2$, yielding the same expression.

With haptic synthesis, the objective is to minimize the creation of spurious energy by increasing the sampling rate as much as required by the device used to produce force and read position. Of course, one special case is when the virtual environment is passive to start with, but it is also possible to consider environments which are not. In any case, what is needed is reduced complexity of the calculations in the closed loop. In the rest of this paper, we will discuss how a number of basic mechanical interactions can be synthesized at little cost. For consistency the notation may differ substantially from that used originally.

2 Friction

In its most basic aspect, friction relates a displacement to a force that tends to oppose it and has at least two distinct states: sticking or slipping. There are velocity dependent effects such as lubrication related effects [3], but these can be ignored. The relation between displacement and force, up to a factor, can be written in differential form using the original Dahl's [1976] model:

$$\frac{\mathrm{d}d}{\mathrm{d}p} = 1 - \zeta\ \mathrm{sgn}(\mathrm{d}p)\,d. \tag{1}$$

This expression is particularly suitable for haptic synthesis since, once Eq. (1) is discretized, for each measured displacement $\bar{p}$ it is easy to find an updated d. The "time free" governing dynamics makes it explicit that velocity is not required and, like real friction, gives a well defined value even if velocity is zero [15]. The state d represents an actual physical quantity: the elastic tangential deflection seen in any real contact. The tangential friction force is then a function of d, say proportionally to the normal force and to a coefficient μ which embodies the properties of a contact (contact geometry, materials and other considerations, see Section 4). That the normal force also results from a deflection will allow us to realize haptic synthesis in general cases without ever to have to worry about interaction forces, as further discussed in Section 4.

However, in the course of implementation we realized that this model gave an unphysical behavior: small movements caused the simulated contact to drift, that is, some bounded inputs under the breakaway threshold gave unbounded net displacement [15]. As a matter of fact, Dahl's model does not admit a sticking phase as commented in [9]. An improved model that retains much of the original simplicity is written:

$$\frac{\mathrm{d}d}{\mathrm{d}p} = 1 - \zeta(d)\,\mathrm{sgn}(\mathrm{d}p)\,d, \tag{2}$$

where $\zeta(d)$ now is a function that governs the transition from stick to slip according to the deflection. Referring to Figure 2, if $\zeta(d) = 0$ for a range of values, then $\mathrm{d}d = \mathrm{d}p$ and hence the contact is stuck. For any other case there will be a mix of elasticity (stick) and plasticity (slip).

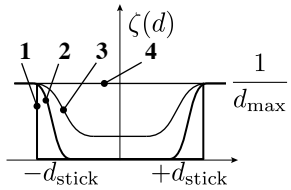

Figure 2: Adhesion functions. **1**) Adequate for haptics. **2**) Better for control of machines [Dupont et al. 02]. **3**) Arbitrary mix of elasticity and plasticity. For **1**, **2**, and **3**, we normally select $d_\mathrm{max} = d_\mathrm{stick}$. If $d_\mathrm{max} < d_\mathrm{stick}$ additional solutions arise. **4**) Dahl: an equal mix of elasticity and plasticity.

This model has many interesting properties but for haptic synthesis, attractive features are ease to specify a vectorial extension and a noise-robust solution. Using boldface to designate vectorial quantities, calling $\bar{\boldsymbol{p}}_k$ the manipulandum's measured position, $\boldsymbol{d}_k$ the elastic component of the displacement, and $\boldsymbol{c}_k$ the plastic component, the online solution is

$$\begin{aligned} \boldsymbol{c}_k &= \begin{cases} \bar{\boldsymbol{p}}_k - \frac{\bar{\boldsymbol{p}}_k - \boldsymbol{c}_{k-1}}{|\bar{\boldsymbol{p}}_k - \boldsymbol{c}_{k-1}|} d_\mathrm{max}, \\ \qquad \text{if } |\bar{\boldsymbol{p}}_k - \boldsymbol{c}_{k-1}| > d_\mathrm{max}; \\ \boldsymbol{c}_{k-1}, \\ \qquad \text{otherwise}, \end{cases} \\ \boldsymbol{d}_k &= \bar{\boldsymbol{p}}_k - \boldsymbol{c}_k \end{aligned} \tag{3}$$

for the simplest version of $\zeta(d)$, the adhesion function **1** in Figure 2. Figure 3 illustrates this computation graphically.

[2] Many similar conditions can be found depending on the assumptions made. For example in Bonneton (1994) approximating e^{-Ts} using the Padé approximation, it was found that conditions for stability were $\mathcal{B} < b + 2M/T$ and $\sigma\mathcal{T} < b + \mathcal{B}$ among others.

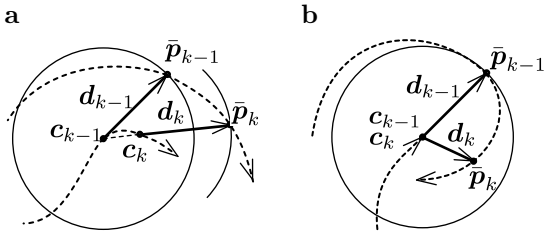

Figure 3: **a**) Sliding state. **b**) Sticking state.

For any adhesion function, the solution can be found by Euler integration:

$$\boldsymbol{c}_k = \begin{cases} \bar{\boldsymbol{p}}_k - \frac{\bar{\boldsymbol{p}}_k - \boldsymbol{c}_{k-1}}{|\bar{\boldsymbol{p}}_k - \boldsymbol{c}_{k-1}|} d_{\max}, \\ \qquad \text{if } \zeta(\bar{\boldsymbol{p}}_k - \boldsymbol{c}_{k-1})|\bar{\boldsymbol{p}}_k - \boldsymbol{c}_{k-1}| > 1; \\ \boldsymbol{c}_{k-1} + \\ |\bar{\boldsymbol{p}}_k - \bar{\boldsymbol{p}}_{k-1}|\zeta(\bar{\boldsymbol{p}}_k - \boldsymbol{c}_{k-1})(\bar{\boldsymbol{p}}_k - \boldsymbol{c}_{k-1}), \\ \qquad \text{otherwise.} \end{cases} \tag{4}$$

The solution can also be vizualized by plotting the vector $\boldsymbol{d}$ while tracing a trajectory with $\boldsymbol{p}$ as input, see Figure 4.

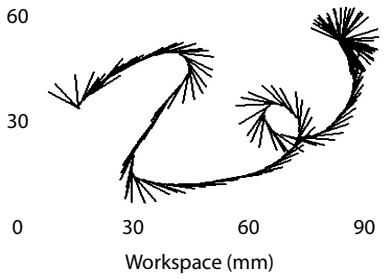

Figure 4: Vector friction $\boldsymbol{d}$ plotted with its origin at $\boldsymbol{p}$. Multiplying by a negative factor proportional to the normal force gives a friction force. The trajectory terminates at the upper right corner in a stuck state where $\boldsymbol{c}$ is invariant, yet $\boldsymbol{d}$ exists.

From the perspective of haptic synthesis, this makes it clear that the simulation of realistic friction is a considerable challenge since the characteristic distance $d_{\max}$—the 'presliding' distance—is measured in micrometers for hard objects. The resolution of the haptic device should be higher than this number to simulate hard contact. Another challenge is related to the passivity of the simulation. During sliding, the model is dissipative by construction, but in the stick phase it is purely elastic. One might think of adding viscosity, but we know that this approach has only limited value. To fix ideas, let's asume that $d_{\max} = 10^{-5}$ m and that the tangential sliding force is 1 N, thus the contact's σ is 10^5 N/m. Therefore, viscosity, real or virtual, for a sampling frequency of 10^4 Hz should be of the order of $\sigma\mathcal{T} = 10$ N·s/m, a large value indeed. This limits how small $d_{\max}$ can be for a given device.

3 Damage

For haptic synthesis, damage is defined as the simulation of the creation of new surfaces in a solid. This may have many forms but we first looked at sharp cutting, basing our model, like that of friction, on basic physical properties [20]. Fracture mechanics indicates that the creation of new surfaces corresponds to the irreversible dissipation of energy proportionally to the area of a crack extension. Cutting is also preceded with storage of elastic energy. In that, it is quite similar to friction. Referring to Figure 5, consider an infinitesimal section of a solid of width dl cut by a sharp blade. As the blade moves by Δd^z, the crack surface is increased by Δs while the crack length extends from c to $c + \Delta c$. If the solid deforms, the solid element surrounding the crack changes from shape R_s to shape $R_{s+\Delta s}$. In the course of a complete cut, our model predicts a number of distinct events.

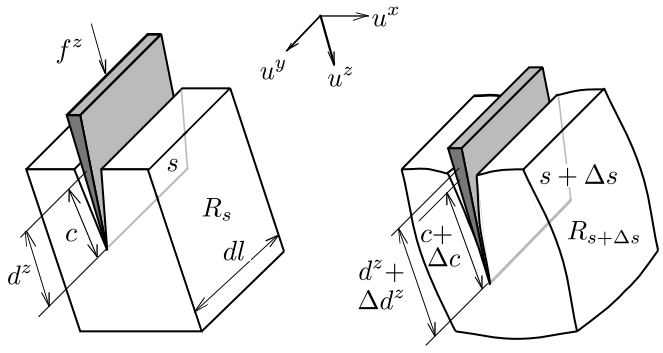

Figure 5: Quantities defined for sharp cutting. A blade move in an elementary block of width dl with a force f^z.

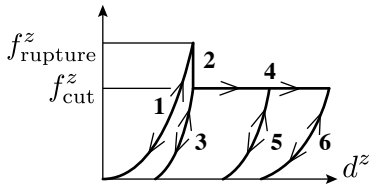

Figure 6: Possible response branches.

These events can be described by reference to Figure 6. As the blade first touches the object, deformation occurs and the response follows path **1** where elastic energy is stored. Deflection continues until the cutting force f^z_{rupture} is sufficient to initiate a crack. Almost instantly, the stored energy is released, **2**, to create a crack whose size can be deduced from the energy stored during initial loading and from the fracture toughness of the material, J_c. If the blade retreats, the response follows another unloading curve **3**, owing to the existence of the crack. If the blade moves forward, sharp cutting occurs. The cutting force f^z_{cut} along **4** can be found from J_c, the movement of the blade and the

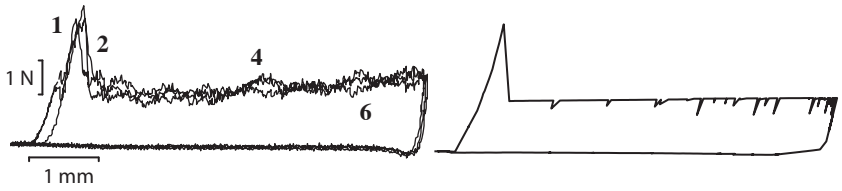

Figure 7: Three overlaid responses from cutting a 20 mm wide potato prism with a sharp razor blade where the response branches are visible. Right: synthesized response.

width of the cut. If at any moment, the blade retreats as in **5** or **6** a new unloading/loading curve is created.

In all cases the force response can be determined from energy conservation considerations involving the work lost in extending a crack, $J_c\, a(\Delta s)$, and the work made by the moving blade, $f^z \Delta d^z$ [20].

Experiments carried out with liver and potato samples indicated good agreement between the model and experiments, see Figure 7. This was further applied to model cutting forces with scissors and other forms of cutting [24, 19]. Please see Chapter **??** in this collection for further detail.

4 Elastic Deformation

When a tool is used to interact with a body without causing damage, deformation occurs. Synthesizing the full, detailed response requires to account for the tool used, the body's shape, material, inhomogeneity, nonlinearity, small and large deformations, support, and so on. These requirements seem to be in opposition with the fact that the fully detailed computational simulation of contact is a formidable computational problem. Experiments where carried out to highlight this [21]. Figure 8 shows a tool ready to indent a sample of liver well supported by a rigid plate. In this condition, the details of the contact mechanics dominate the response. Figure 8 shows the response for two different tools. Changing the tool size (same shape) by a factor 4 modifies the response by orders of magnitude for the same indentation.

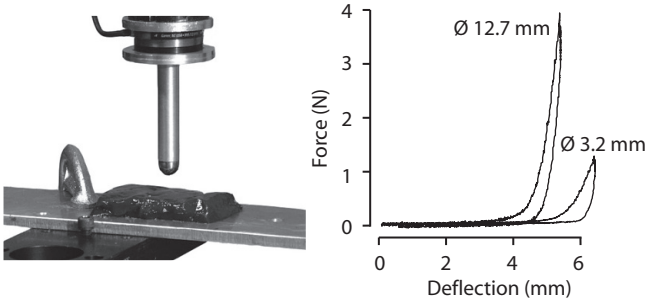

Figure 8: Testing a well supported sample of liver and response to local deformation of biological tissue with two different tools. After a few millimeters of deflection the responses differ by orders of magnitude.

Similar significant differences would be observed in bodies which are homogenous or not, isotropic or not, whether deformation is small or large, local or global, etc. [22]. In this reference, we list four requirements for high-fidelity haptic simulation:

1. resemblance of virtual force responses with actual responses,
2. force continuity under all allowed maneuvers,
3. passivity of the virtual environment, and
4. high update rate.

Haptic synthesis techniques, however, allows one to account for the full complexity of mechanical interactions with deformable bodies while meeting these requirements. The basic observation is that when a given tool encounters a given body, no matter how complicated the interaction is, the subsequent response is entirely determined by the initial point of contact. If we consider that for a given tool each point of the surface determines a different response—a vector function of a deflection vector—, then the entire response is nothing but a continuous field of functions. From physics, we know that each of these functions should be conservative and so must be the field. This observation allowed us to establish a synthesis method to reconstruct passively this field from a finite set of samples [23].

Briefly, the method consists of interpolating a finite set of vector functions determined from first principles, from measurements, or from offline simulations. Referring to Figure 9, one approach is to store one function at each surface node of the synthesized body and interpolate a new response function for initial contact point $\boldsymbol{c}$ given a deflection $\boldsymbol{d}$.

Because these functions are nonlinear, the choice of coordinates is crucial and a new set must be interpolated at $\boldsymbol{c}$ from the coordinates used for each node. For the case indicated in Figure 9, there are three coordinates, $\nu \in \{x, y, z\}$. For any patch m, with the interpolation weights ${}^m n_i(c)$ the interpolation formulae are:

$$u_c^\nu = \sum_{i=1}^{3} {}^m n_i(c)\ {}^m u_i^\nu, \tag{5}$$

$$f_c^\nu(d^\nu) = \sum_{i=1}^{3} {}^m n_i(c)\ {}^m f_i^\nu(d^\nu). \tag{6}$$

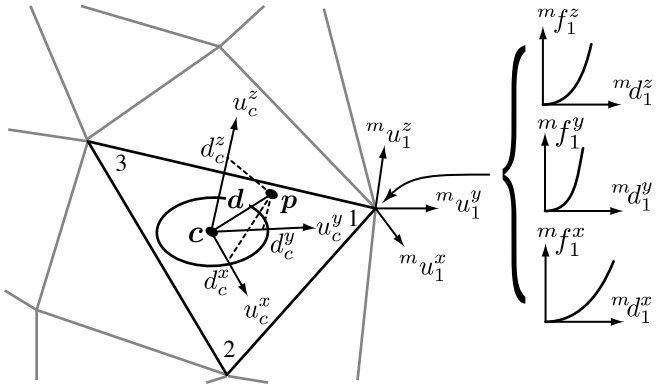

Figure 9: Local response encoded as force deflection curves at each node. If the projection of point $\boldsymbol{p}$ is within a set bound, the contact is stuck.

The synthesis of the nonlinear response is a simple process which can be decoupled from the other processes in a complete simulation system. In particular, interference detection which reduces to the determination of an 'active patch', can be performed asynchronously. The algorithmic details are in [23]. Moreover the storage required for many cases of practical interest is quite modest owing to necessity to store data proportionally to the surface of the body, but not to its volume. Now, if the interaction has a lateral component, then slip can occur and therefore the point $\boldsymbol{c}$ could be moving.

In Section 2, we developed a synthesis model for the dynamics of sliding contacts. Following this model, the movement of point $\boldsymbol{c}$ can be governed by the algorithm described there. In effect, the projection of point $\boldsymbol{p}$ on the envelop of the undeformed body should remain within bounded lateral deflections. We have seen earlier that for hard objects, this lateral deflection could be as small as a few micrometers, but for deformable bodies such as organs, it can be as large as centimeters. The basic phenomenon is nevertheless the same so the synthesis method outlined here can be viewed an extension of the simple model of Section 2, but accounting for shape, normal deflection, tool and material properties. The dependence of the tangential friction force as a function of the normal component can be expressed by a friction coefficient defined as:

$$\mu_c = \frac{d_c^z}{\sqrt{{d_c^x}^2 + {d_c^y}^2}} \tag{7}$$

Coefficient μ_c may be known at only a finite number of places on the surface of the body and be interpolated to be defined everywhere. Moreover, if μ_c is made to be invariant with the contact surface, that is, with the normal deflection, then it is equivalent to assuming that Amontons' Law holds [23].

It is is also possible to synthesize a difference response for different manners in which a tool can contact a body. If m is a patch on the body and j a specific response:

$$u_c^\nu = \sum_i {}^j n_i(c) \left(\sum_l {}^m n_l(c)\, {}^{jm} u_{il}^\nu \right), \tag{8}$$

$$f_c^\nu(d^\nu) = \sum_i {}^j n_i(c) \left(\sum_l {}^m n_l(c)\, {}^{jm} f_{il}^\nu(d^\nu) \right). \tag{9}$$

The techniques described up to now can be combined in a unified framework for the haptic synthesis of a wide range of effects [19].

5 Texture

Texture refers to small-scale modifications of mechanical interaction response during scanning or during penetration. In Campion and Hayward [2005] we observed that textural synthesis could be viewed as a small oscillatory component superposed to a low frequency nominal response component, see Figure 10. This small oscillatory component can be combined with any synthesized signal, for example, adding it to the synthesized response of Figure 7 would increase realism. Thus, texture synthesis is amenable to 'small signal analysis'. Using the analogy between scanning a texture and a wave traveling at a variable speed, we used the Nyquist and the Courant conditions to derive relationships that state the conditions under which a texture can possibly be synthesized by a haptic device—a mechanical system which no longer should be approximated by a rigid body.

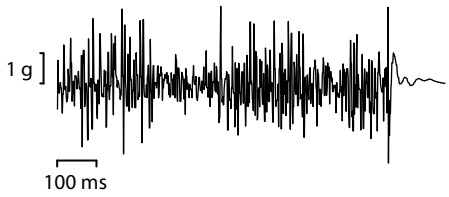

Figure 10: Acceleration of a stylus dragged on a wooden surface.

The summary of these derivations is given here. Given k the spatial frequency of a grating, $\mathcal{T}$ the system sampling period, v the scanning velocity, δ the device resolution, b the force resolution, α a temporal safety factor (at least 2, better 10), β a spatial safety factor (at least 2, better 10), γ a force reconstruction safety factor (at least 10), A the desired force amplitude the rendered grating, A_0 the maximum control stiffness, and F_0 the first mode of the device, then Table 1 summarizes the limits that cannot be exceeded in order to make it possible to render a given grating with a given device. These limits do not guarantee that the grating question will be rendered correctly, but if one of these limits is exceeded it is highly likely that it will not be the case. We also found that the the limit A_0 was proportional to the slope of the texture function, or more generally to

the norm of the Jacobian matrix of the texture generating function is it is multidimensional.

Table 1: Summary of limits.

Scanning velocity limit	$\alpha\, k\, v\, \mathcal{T} < 1$
Low speed reconstruction limit	$\beta\, k\, \delta < 1$
High speed reconstruction limit	$\alpha\, k\, \delta < 1$
Force reconstruction limit	$\gamma\, b < A$
Gain limit	$A\, k < A_0$
Device structural limit	$v\, k < F_0$

As an example, the PHANTOM which, in principle, has enough resolution in time and space to render correctly textures up to 1 mm in spatial frequency was experimentally found to incorrectly render textures as coarse as 10 mm because of mechanical resonances with a first anti-resonance as low as 30 Hz. With another device, the Pantograph, which has a much higher structural bandwidth, 400 Hz, it was possible to find a reconstruction filter which robustified the system under all reasonable operating conditions, although finding optimal filters that can take into account the open loop and the closed loop behavior of a given haptic system remains open question.

6 Shocks

When a tool meets an object with significant initial velocity, a shock occurs. The response is an important part of the feel. In this Section we look at a synthesis model which accounts for a transient response. For more realism decaying oscillatory components may be added [25]. Shocks have the particularity that they can be synthesized in "open-loop", that is momentarily ignoring the measured position of the device during the duration of the event [18]. For more detail, the reader should refer to Chapter **??** in this collection.

The model adopted is a simplified version of the Hertz' contact theory. It says that when objects are in contact, there is a finite contact area that increases with mutual, or one-sided local deformation. At the same time, some energy is lost during the brief moment of a collision. Some of it is lost through internal dissipation, some is lost in acoustic propagation. It is clearly very difficult to predict exactly these effects, however, a good phenomenological description is captured by this force response equation known as the Hunt-Crossley collision model [17]:

$$f_{\text{shock}} = K(d^z) - D(d^z)\dot{d^z}, \tag{10}$$

where d^z is, as before, the penetration depth at the contacting surface, and $K(\cdot)$ can be a response of the form $k_0\, d^{z\,i}$ where i may represent the growth rate of the surfaces in contact. The function $D(\cdot)$ is meant to represent the details of dissipation. For example, if we take the simplest case of $D(d^z) = B_0\, d^z$, it expresses the fact that when the area in the contact increases with d^z, the dissipative coefficient also increases. It also expresses the fact that when $d^z = 0$, just at the beginning of a collision, $f_{\text{shock}} = 0$ also, because there is no dissipation. This guarantees force continuity since the force is also zero just before the collision. Various profiles for $K(\cdot)$ and $D(\cdot)$ provide for different collision "feels". An open-loop implementation can be accomplished by equating Eq. (10) to $-m\,\ddot{d^z}$ where m is a virtual mass which can be selected to be close of the effective end-point inertia of the device. Solving the resulting differential equation inexpensively using Euler integration for a short time interval, from the instant the collision is detected to the time d^z is again zero, give a force trajectory that can be played in open-loop and which necessarily terminates with a value of the force equal to zero. Even a crude estimate of the initial value of $\dot{d^z}$ will give a realistic sensation.

Methods exist for identifying $K(\cdot)$ and $D(\cdot)$ but their description is beyond the scope of this paper. In an any case an important model matching condition is established when the *loop areas* are equal between measurements and simulation, that is, when the dissipation is the same. This model matching condition appears to be more important that attempting to reproduce the details of the loop shapes.

As mentioned earlier, on impact, objects can have a structural response which can be synthesized by a sum of decaying sinusoidal vibrations, that is by modal synthesis $f_{\text{vib}} = \sum_i e^{b_i t} a_i \sin(\omega_i t)$. A structural shock can be initiated as a response to an event. Computationally, the response may be generated from a wave table. Other methods can be used to specify a waveform which is played during the duration of a simulated shock. In any case, the magnitude of the shock is modulated by a factor which depends on the initial contact velocity.

7 Conclusion

Haptic synthesis bears some analogy with realtime audio synthesis where a computational loop must be able to reconstruct physically and perceptually relevant aspects of the original signal. What our experience has shown is that in many cases, unlike the case of audio synthesis, the limits dues to the performance characteristics of currently available devices far exceed the limits due to computation [16].

This state of affairs calls for new approaches in the design of devices, e.g. [14, 13] among others, with significantly improved performance characteristics that can take full advantage of the currently available computational techniques of haptic synthesis, in addition to those presently under development. In our laboratory, these are specifically targeted at accurately synthesizing dynamics effects such as impact, viscosity and others.

References

[1] J. J. Abbott and A. M. Okamura. Effects of position quantization and sampling rate on virtual wall passivity. *IEEE Transactions on Robotics*, 21(5):952–964, 2005.

[2] R. J. Adams and B. Hannaford. Stable haptic interaction with virtual environments. *IEEE Transactions on Robotics and Automation*, 15(3):465–474, 1999.

[3] B. Armstrong-Hélouvry, P. Dupont, and C. Can udas De Wit. A survey of models, analysis tools and compensation methods for the control of machines with friction. *Automatica*, 30(7):1083–1138, 1994.

[4] B. Bonneton. Pantograph project, chapter: Implementation of a virtual wall. Technical report, Center for Intelligent Machines, McGill University, 1994.

[5] G. Campion and V. Hayward. Fundamental limits in the rendering of virtual haptic textures. In *Proceedings First Joint Eurohaptics Conference and Symposium on Haptic Interfaces for Virtual Environments and Teleoperator Systems WHC'05*, pages 263–270, 2005.

[6] J. E. Colgate and G. Schenkel. Passivity of a class of sampled-data systems: Application to haptic interfaces. In *Proceedings American Control Conference*, pages 37–47, 1994.

[7] P. Dahl. Solid friction damping of mechanical vibrations. *AIAA Journal*, 14(2), 1976.

[8] N. Diolaiti, G. Niemeyer, F. Barbagli, and J. K. Salisbury. Stability of haptic rendering: Discretization, quantization, time delay, and coulomb effects. *IEEE Transactions on Robotics*, 22(2):256–268, 2006.

[9] P. Dupont, B. Armstrong, and V. Hayward. Elasto-plastic friction model: Contact compliance and stiction. In *Proceedings American Control Conference*, pages 1072–1077, 2000.

[10] P. Dupont, V. Hayward, B. Armstrong, and F. Altpeter. Single state elasto-plastic friction models. *IEEE Transactions on Automatic Control*, 47(5):787–792, 2002.

[11] R.E. Ellis, N. Sarkar, and M. A. Jenkins. Numerical methods for the force reflection of contact. *ASME Transactions on Dynamic Systems, Modeling, and Control*, 119(4):768–774, 1997.

[12] B. Gillespie and M. Cutkosky. Stable user-specific rendering of the virtual wall. In *Proceedings of the ASME International Mechanical Engineering Conference and Exposition*, volume DSC-Vol. 58, pages 397–406, 1996.

[13] A. H. Gosline, G. Campion, and V. Hayward. On the use of eddy current brakes as tunable, fast turn-on viscous dampers for haptic rendering. In *Proceedings of Eurohaptics*, pages 229–234, 2006.

[14] W. S. Harwin and S. A. Wall. Mechatronic design of a high frequency probe for haptic interaction. In *Proceedings 6th International Conference on Mechatronics and Machine Vision in Practice*, pages 111–118, 1999.

[15] V. Hayward and B. Armstrong. A new computational model of friction applied to haptic rendering. In P. Corke and J. Trevelyan, editors, *Experimental Robotics VI*, volume 250 of *Lecture Notes in Control and Information Sciences*, pages 403–412, 2000.

[16] V. Hayward and O. R. Astley. Performance measures for haptic interfaces. In G. Giralt and G. Hirzinger, editors, *Robotics Research: The 7th International Symposium*, pages 195–207, Heidelberg, 1996. Springer Verlag.

[17] K. H. Hunt and F. R. E. Crossley. Coefficient of restitution interpreted as damping in vibroimpact. *ASME Journal of Applied Mechanics*, 42(2):440–445, 1975.

[18] K. J. Kuchenbecker, J. Fiener, and G. Niemeyer. Improving contact realism through event-based haptic feedback. *IEEE Transactions on Visualization and Computer Graphics*, 12(2):219–230, 2006.

[19] M. Mahvash. A novel approach for modeling separation forces between deformable bodies. *IEEE Transactions on Information Technology in Biomedecine*, page In press, 2006.

[20] M. Mahvash and V. Hayward. Haptic rendering of cutting: A fracture mechanics approach. *Haptics-e*, 2(3):, 2001.

[21] M. Mahvash and V. Hayward. Haptic rendering of tool contact. In *Proceedings of Eurohaptics*, pages 110–115, 2002.

[22] M. Mahvash and V. Hayward. High fidelity haptic synthesis of contact with deformable bodies. *IEEE Computer Graphics and Applications*, 24(2):48–55, 2004.

[23] M. Mahvash and V. Hayward. High fidelity passive force reflecting virtual environments. *IEEE Transactions on Robotics*, 21(1):38–46, 2005.

[24] M. Mahvash and A. Okamura. A fracture mechanics approach to haptic synthesis of tissue cutting with scissors. In *First Joint Eurohaptics Conference and Symposium on Haptic Interfaces for Virtual Environment and Teleoperator Systems*, pages 356–362, 2005.

[25] A. Okamura, J. T. Dennerlein, and R. D. Howe. Vibration feedback models for virtual environments. In *Proceedings of IEEE International Conference on Robotics and Automation*, volume 3, pages pp. 2485–2490, 1998.

[26] K J. Salisbury, D. Brock, T. Massie, N. Swarup, and C. Zilles. Haptic rendering : Programming touch interaction with virtual objects. In *Proceedings Symposium on Interactive 3D Graphics*, pages 123–130, New York, NY, USA, 1995. ACM Press.